

FIG. 1. Characterization of muscle tissue probes. Panel A shows a representative enzyme histochemical preparation from non-diabetic (left) and diabetic (right) m. gastrocnemius ($\times 100$). The tissue was stained with myofibrillar ATPase (pH 9.4). The bright cells are type I red muscle fibers, and the dark cells are type II white muscle fibers. The pictures show neurogenic atrophy according to peripheral vascular neuropathy with grouped atrophy especially in type II fibers, type-grouping of the type I fibers. Panel B shows histograms of square sections of m. gastrocnemius from non-diabetic (left, $n = 8$) and diabetic patients (right, $n = 9$). Means \pm S.D. of each square dimension class for red and white muscle fibers are shown. Panel C shows a comparison of total square section from the histogram depicted in panel B for non-diabetic (N) and diabetic (D) m. gastrocnemius with that derived from normal fiber composition of m. lattissimus dorsi (L) as published in Ref. 50.

TABLE II

Muscle enzyme activities and non-collagen protein (NCP) levels for patients admitted into the study

The enzyme activities were measured twice for each patient as described under "Experimental Procedures." The units of activity were normalized for non-collagen protein. Muscle probes which revealed activities which were not within the given ranges were excluded from further characterization of the receptor kinase.

Enzyme	Nondiabetic muscle	NIDDM muscle
	units/g NCP	units/g NCP
Lactate dehydrogenase	1040 ± 290	1070 ± 340
Phosphofructo kinase	150 ± 40	155 ± 30
Phosphoglycerate kinase	880 ± 200	910 ± 270
Phosphoglucomutase	975 ± 175	1060 ± 260
	mg/g muscle	mg/g muscle
NCP	76 ± 16	72 ± 10

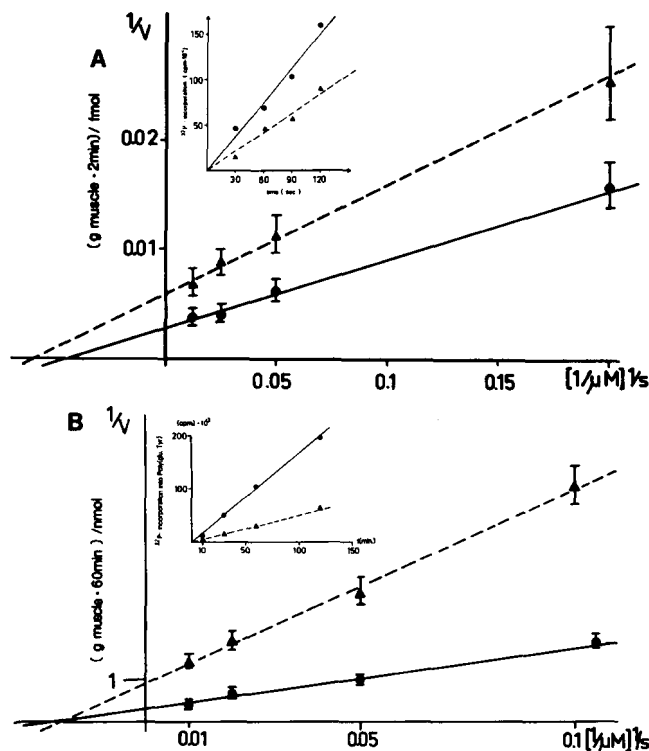


FIG. 6. Kinetic data for autophosphorylation and substrate phosphorylation activity. Panel A, a Lineweaver-Burk plot showing the relation between autophosphorylation and ATP concentration for control (●) and diabetic (▲) receptors. These data were obtained during a 2-min incubation, during which time autophosphorylation was linear (inset). Panel B, a Lineweaver-Burk plot showing the phosphorylation of poly(Glu:Tyr 4:1) by the control (●) and diabetic (▲) receptor as a function of poly(Glu:Tyr) concentration. These data were obtained as described in the method section for a time period of 60 min, during which the phosphorylation was linear (inset). Mean ± S.D. are presented for the data of all patients in group I (●) and group II (▲).

the regulatory region or the C terminus do not play a direct role in activation, as previously suggested (51, 53).

DISCUSSION

The insulin receptor kinase isolated from the skeletal muscle of NIDDM patients exhibits *in vitro* a reduced insulin sensitivity and responsiveness (32-34). Our results agree in general with the findings in human fat (31) and liver cells (54) of type II diabetic patients and suggest that a kinase abnormality might contribute to the pathogenesis of insulin

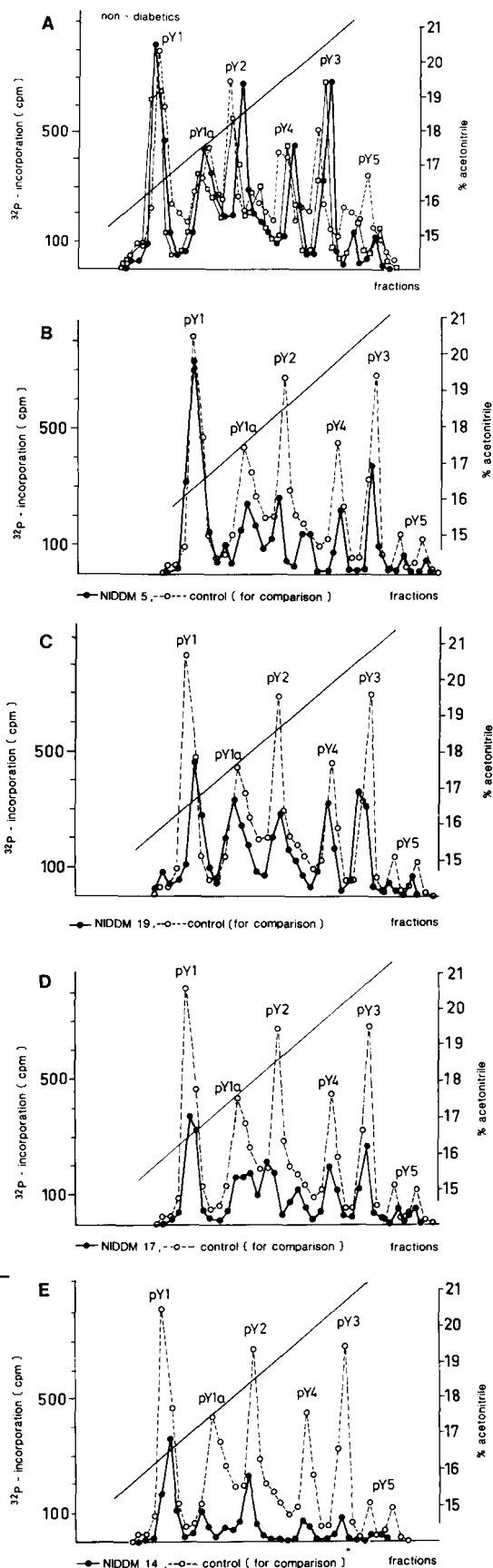


FIG. 7. HPLC-profiles of tryptic peptides from several non-diabetic (A) and diabetic receptors (B-E). Equal amounts of insulin receptor were phosphorylated for 10 min during insulin stimulation (controls, 100 nM and diabetic 1000 nM), and processed as described under "Experimental Procedures." About 94% of the radio-

Autoactivation of Type II Diabetic Insulin Receptors

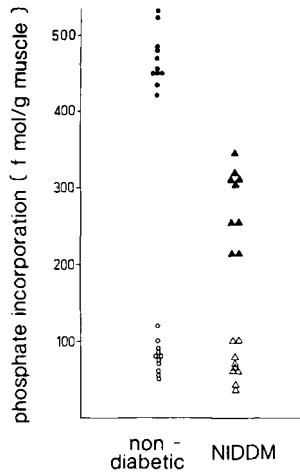


Figure 4. Phosphate incorporation into the 95 kDa β -subunit of the insulin receptor of each patient from group I and II, and of each preparation for group III. Autophosphorylation was carried out as described in Fig. 3 and under experimental procedures and total phosphate incorporation was calculated for the basal and maximal stimulated probes (10^{-7} or 10^{-8} M insulin) (controls: basal (○) and maximal stimulation (●); NIDDM: basal (△) and maximal stimulation (▲)).

In order to detect possible influences of age, localization of the muscle, influences of the surgical technique or undetected arteriovascular disease, we studied the insulin receptor kinase of musculus latissimus dorsi of the group III patients. The maximal 32 P-phosphorylation was within the range of the non-diabetic control group I. These values are included in Fig. 4 with the group I controls. Furthermore, the dose response and the maximal 32 P-incorporation of the kinase isolated from the gastrocnemius of the 8 patients of group I was identical with the dose response found for the kinase isolated from the musculus latissimus dorsi of the younger patients of group III (data not shown). These values also agreed with previously published results (45). Therefore, in addition to the morphological and enzymatic examination of the tissue samples (Fig. 1, Table 2), the results with group III further exclude nonspecific effects due to the surgical technique, the age of the patients, the muscle localization and the immobilization of hospitalized patients.

Kinetic properties of the insulin receptor kinase—The kinase activity of the insulin receptor purified from muscle of NIDDM patients was significantly less than the activity of the control during assays with poly(Glu:Tyr 4:1). Similar to the autophosphorylation activity, poly(Glu:Tyr) phosphorylation during maximal insulin stimulation was reduced about 50–80% (Fig. 5). Although basal autophosphorylation was similar for control and NIDDM receptors, a significant difference was detected for basal phosphorylation of poly(Glu:Tyr).

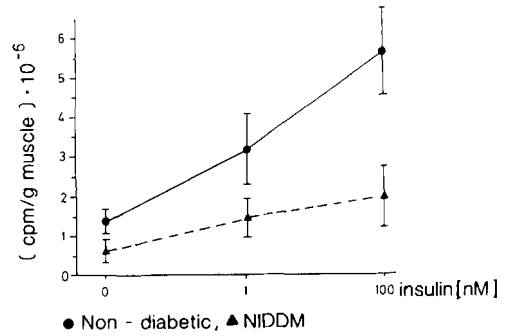


Figure 5. Insulin dose-response curve of poly(Glu:Tyr 4:1) phosphorylation for group I non-diabetic (●) and group II diabetic receptors (▲). The substrate phosphorylation assay was carried out with each muscle sample as described under experimental procedures for 1 h using 1.8 nM poly(Glu:Tyr 4:1). The kinase activity was measured in the absence of insulin, and at 1 and 100 nM insulin using equal amounts of insulin receptor as determined by insulin binding. The average activity (\pm SD) for each group (Table 1) is shown. The coefficient of variability for the assay using the same receptor was 5%.